

Lithium ion batteries cathode material: V_2O_5

Baohe Yuan(袁保合), Xiang Yuan(袁祥), Binger Zhang(张冰儿), Zheng An(安政), Shijun Luo(罗世钧), and Lulu Chen(陈露露)

Citation: Chin. Phys. B, 2022, 31 (**3**): 038203. DOI: 10.1088/1674-1056/ac21be
Journal homepage: http://cpb.iphy.ac.cn; http://iopscience.iop.org/cpb

What follows is a list of articles you may be interested in

DFT study of solvation of Li^+/Na^+ in fluoroethylene carbonate/vinylene carbonate/ethylene sulfite solvents for lithium/sodium-based battery

Qi Liu(刘琦, Guoqiang Tan(谭国强), Feng Wu(吴锋), Daobin Mu(穆道斌), and Borong Wu(吴伯荣)
Chin. Phys. B, 2021, 30 (**3**): 038203. DOI: 10.1088/1674-1056/abd763

Comparative calculation on Li^+ solvation in common organic electrolyte solvents for lithium ion batteries

Qi Liu(刘琦), Feng Wu(吴锋), Daobin Mu(穆道斌), Borong Wu(吴伯荣)
Chin. Phys. B, 2020, 29 (**4**): 048202. DOI: 10.1088/1674-1056/ab75cc

Gas treatment protection of metallic lithium anode

Wen-jun Li(李文俊), Quan Li(李泉), Jie Huang(黄杰), Jia-yue Peng(彭佳悦), Geng Chu(褚赓), Ya-xiang Lu(陆雅翔), Jie-yun Zheng(郑杰允), Hong Li(李泓)
Chin. Phys. B, 2017, 26 (**8**): 088202. DOI: 10.1088/1674-1056/26/8/088202

Conductivity and applications of Li-biphenyl-1, 2-dimethoxyethane solution for lithium ion batteries

Geng Chu(褚赓), Bo-Nan Liu(刘柏男), Fei Luo(罗飞), Wen-Jun Li(李文俊), Hao Lu(陆浩), Li-Quan Chen(陈立泉), Hong Li(李泓)
Chin. Phys. B, 2017, 26 (**7**): 078201. DOI: 10.1088/1674-1056/26/7/078201

Instability of lithium bis(fluorosulfonyl)imide (LiFSI)–potassium bis(fluorosulfonyl)imide (KFSI) system with $LiCoO_2$ at high voltage

Zhang Shu, Li Wen-Jun, Ling Shi-Gang, Li Hong, Zhou Zhi-Bin, Chen Li-Quan
Chin. Phys. B, 2015, 24 (**7**): 078201. DOI: 10.1088/1674-1056/24/7/078201

REVIEW

Lithium ion batteries cathode material: V_2O_5

Baohe Yuan(袁保合)[†], Xiang Yuan(袁祥), Binger Zhang(张冰儿), Zheng An(安政), Shijun Luo(罗世钧), and Lulu Chen(陈露露)[‡]

North China University of Water Resources and Electric Power, Zhengzhou 450011, *China*

(Received 10 July 2021; revised manuscript received 19 August 2021; accepted manuscript online 27 August 2021)

Among all the known electrode materials, vanadium pentoxide (V_2O_5) has high reversible capacity. It is a very valuable material for research of the complexity, rich structure and morphology. However, it also has some disadvantages, such as poor cycle stability, low discharge voltage, low conductivity and Li^+ diffusion coefficient. In this regard, researchers have carried out a lot of research, such as using various methods to improve the nanostructures, introducing heterostructures, introducing point defects or cation doping in the crystal structure, etc. The electrochemical performance of V_2O_5 has been significantly improved in reversible capacity, high-rate capacity and long-term cycle stability. In this paper, V_2O_5 based nanostructure with different chemical composition are briefly introduced, and it covers V_2O_5 nanomaterials with different morphology, including 1D nanorods, nanobelts, nanotubes, 2D leaf like nanosheets and other nanosheets, and 3D hollow structures, porous nanostructures, porous eggshell microsphere structures. The composite nanomaterials of V_2O_5 and different carbonaceous supports are also introduced. Finally, the V_2O_5 composite materials doped with cations are discussed. The electrochemical performance of V_2O_5 based electrode can be improved effectively by obtaining appropriate nanostructure and optimized chemical composition.

Keywords: lithium ion battery, V_2O_5 nanostructures, electrochemical properties, nanotubes and nanowires

PACS: 82.47.Aa, 79.60.Jv, 65.40.gk **DOI:** 10.1088/1674-1056/ac21be

1. Introduction

In recent years, due to the shortage of traditional fossil energy and concerns about greenhouse gas emissions, it has become extremely important to make more effective use of energy and save limited energy in the world. At present, scientists and engineers are looking for renewable and more efficient strategies to create and store energy, so as to reduce or even avoid the impact on the environment, such as energy collected from solar heating,[1] photovoltaic power generation,[2] nuclear fission and fusion,[3] wind power generation,[4] hydropower generation,[5] and tidal fluctuation.[6] Biomass and geothermal energy[7] are favorable alternatives to traditional fossil fuel combustion.[8] More and more reports of scientific breakthroughs and technological innovation are given. The development of advanced energy storage technology is very important to solve the energy problem. Therefore, it is urgent to need long-life, low-cost and environmental protection reliable batteries to meet the key energy storage needs of modern society. Since Sony firstly commercialized lithium ion battery (LIB) in 1991, because of its high energy density and high safety, it has been widely used in consumer electronics and many other fields. In more than a quarter of a century, LIB has become a popular, portable and rechargeable secondary battery, and it has a wide range of applications, such as personal electronic devices, electric vehicles, hybrid electric vehicles and smart grid [9] However, the electrochemical performance of LIBs still needs to be improved. The preparation of new reliable electrode materials plays an important role in the further development of LIBs.

The lithium ion battery consists of positive electrode, negative electrode, separator, electrolyte and battery shell. In the process of charging and discharging, lithium ions are insertion and extraction between the two electrodes: during charging, lithium ions are deintercalated from the positive electrode and embedded into the negative electrode through the electrolyte, and the negative electrode is in a lithium rich state; the opposite is true when discharging.[10] Its working principle is shown in Fig. 1. In general, the working principle of LIB depends on the movement of lithium ions between the positive and negative electrodes. In lithium ion battery, the insertion/extraction process of lithium ion between cathode layers is a diffusion process, so it is very important in the design of its structure. Larger grain size and anisotropic crystallization are not conducive to the intercalation process, while smaller grain size and spherical shape are beneficial to shorten the diffusion distance of lithium ion in the host, thus increasing the diffusion rate of lithium ion.

As an important part of lithium ion batteries, cathode materials directly affect the performance of lithium ion batteries. The common cathode materials for LIBs mainly include $LiCoO_2$,[11] $LiNiO_2$,[12] $LiMn_2O_4$/$LiMnO_2$,[13,14] $LiFeO_4$,[15] $Li(NiCoMn)O_2$,[16] etc., and the comparison of several kinds of cathode materials for LIBs is shown in Table 1. Their theo-

[†]Corresponding author. E-mail: yuanbaohe@ncwu.edu.cn
[‡]Corresponding author. E-mail: chenlulu@ncwu.edu.cn

© 2022 Chinese Physical Society and IOP Publishing Ltd

retical capacity is low, the cost of $LiCoO_2$ and $LiNiO_2$ is high, and especially the preparation conditions of $LiNiO_2$ are quite harsh. Although a new layered manganese oxide ($LiMnO_2$) has been developed in recent years, it still has the problem of structural instability in the process of charging and discharging. The voltage platform of $Li(NiCoMn)O_2$ battery is high, and its safety performance is poor. Therefore, the research on cheap and high-performance cathode materials has become the focus of LIB industry.

Vanadium is a very common transition metal, which has four oxidation states of V^{2+}, V^{3+}, V^{4+}, V^{5+}, and vanadium is one of the most abundant elements in the earth.[17] V_2O_5 is the most common vanadium oxide and the most stable form in the vanadium oxide family. Among all known cathode materials, V_2O_5 has very high reversible capacity. Its complexity, rich structure and morphology make it an amazing material for LIB. The theoretical specific capacity of V_2O_5 with twice lithium ion deintercalation is about 294 mAh/g, while that of V_2O_5 with three times lithium ion deintercalation is about 441 mAh/g, this is much higher than the capacity of commonly used cathode materials. V_2O_5 is a typical interlaminar compound, each layer is combined by van der Waals force. Due to the weak van der Waals force between adjacent layers, V_2O_5 is prone to various phase transitions, such as α, ε, δ, γ, and ω phase, and the specific phase depends on the degree of lithium ion intercalation. In the actual lithium ion insertion process, that is, during the discharge process of LIB, the reaction from α phase to ω phase is related to the potential drop of Li/Li^+.[17] On the other hand, the reverse reaction process from γ phase to α phase occurs when lithium ions are delaminated from $Li_xV_2O_5$ and a rising voltage is applied, and sometimes the formation of ω-$Li_xV_2O_5$ phase is irreversible.[17]

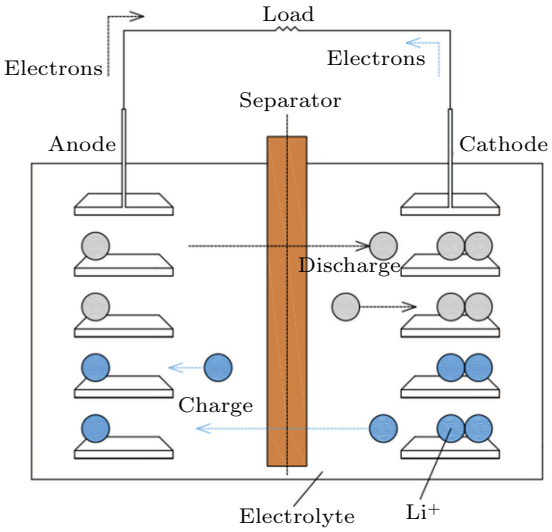


Fig. 1. Schematic diagram of charging and discharging process of LIB.

Table 1. Comparison of several kinds of cathode materials for LIBs.

Cathode materials	Lithium manganate oxide		Lithium cobaltite oxide	Lithium nickel oxide	Ferrous lithium phosphate	Lithium nickel cobalt manganese oxide
Main components	$LiMn_2O_4$[14]	$LiMnO_2$[13]	$LiCoO_2$[11]	$LiNiO_2$[12]	$LiFeO_4$[14]	$Li(NiCoMn)O_2$[15]
Theoretical capacity (mAh/g)	148	286	274	274	170	280
Actual capacity (mAh/g)	100–120	200	135–145	190–210	130–140	> 150
Operating voltage (V)	3.1–3.9	3.4–4.3	2.5–4.1	2.5–4.1	3.2–3.7	2.5–4.4
Cycle performance	$> 500^{th}$	poor	$> 300^{th}$	poor	$> 2000^{th}$	$> 800^{th}$
Safety	good	good	poor	poor	good	poor

Although V_2O_5 is considered to be a promising cathode material for LIBs, it also has some disadvantages, such as poor cycle stability, low discharge voltage, low conductivity and lithium ion diffusion coefficient. In the past few decades, researchers have carried out many results, such as relying on the preparation and doping of nanomaterials, the introduction of heterostructures and point defects in crystal structure.[18] The introduction of structural defects has a great influence on the electrochemical performance of V_2O_5, such as electrochemical capacity, reactivity, conductivity and alkali ion transport.[17] These structural defects can be used as nucleation centers in the process of insertion/extraction, thus increasing the cycle performance. However, how to accurately adjust the defect location and stabilize the long-term cycle structure remains to be solved. The structure of nanomaterials can shorten the diffusion path length of ions and electrons, and increase the surface area of insertion/extraction reaction effectively, while heterostructures and cation doping can reduce electrode polarization, significantly improve conductivity and cycle stability.[17] The key of these methods is to enhance the ionic and electronic conductivity and structural stability of V_2O_5. Therefore, when V_2O_5 is used as electrode material, the reversible capacity, high-rate capacity and long-term cycle stability are significantly improved.

This paper introduces the synthesis methods of V_2O_5 based nanomaterials with different structures and chemical compositions, which covers V_2O_5 nanomaterials with different morphology, including 1D nanorods, nanobelts, nanotubes, 2D leaf like nanosheets and other nanosheets, and 3D hollow structures, porous nanostructures, porous eggshell microsphere structures. The composite nanomaterials of V_2O_5 and different carbonaceous supports (such as graphene, carbon nanotubes and reticular porous carbon matrix) are also introduced. Finally, the V_2O_5 composite materials doped with

cations are discussed. This paper is to provide a more in-depth and reasonable understanding of how to effectively improve the electrochemical performance of V_2O_5 based electrode by obtaining appropriate nanostructures and optimized chemical composition.

2. Nanostructured V_2O_5

The preparation of nanomaterial has great influence on the electrochemical performance of V_2O_5. It is generally considered that reducing the particle size is one of the most influence for the electrochemical performance of materials. The unique properties of nanomaterials lie in their large specific surface area and good structural properties. The transmission length of electrons and lithium ions will be shortened in nanomaterials, the contact area between electrode and electrolyte will be increased, and it can adapt to the strain of Li^+ insertion/extraction in nanomaterials. Table 2 summarizes the electrochemical properties of V_2O_5 as a cathode material for various 1D, 2D and 3D nanostructures.

Table 2. Electrochemical performance of 1D, 2D, 3D nanostructured V_2O_5 for LIB cathode materials.

Precursor material	Nano structures	Initial capacity (mAh/g)	Current density (mA/g)	Cycles (times)	Capacity (mAh/g)	References
V_2O_5 powder	Nanorod	274	14.7	30	213	[19]
NH_4VO_3	Nanobelt	240	294	100	211	[20]
NH_4VO_3	Nanorod	212	294	100	163	[21]
V_2O_5 powder	Nanobelt	142	50	100	137	[22]
NH_4VO_3	Nanobelt	155	1470	300	102	[25]
V_2O_5 powder	Nanosheet	237	500	100	203	[27]
NH_4VO_3	Nanosheet	259	100	200	209	[28]
V_2O_5 powder	Nanosheet	291	59	50	276	[29]
V_2O_5 powder	Nanosheet	330	100	50	240	[30]
Ammonia metavanadate	Nanobelt membrane	293	500	50	237	[31]
NH_4VO_3	Hollow porous structure	285	100	60	213	[32]
NH_4VO_3	Hollow microspheres	449	1000	100	406	[35]
V_2O_5 powder	Porous hierarchical microspheres	147	147	30	136	[36]
NH_4VO_3	Porous microspheres	287.2	50	50	225.7	[37]
NH_4VO_3	Hollow spheres	273	58.8	50	189	[38]

2.1. The 1D nanostructure

Pan *et al.* prepared V_2O_5 nanorods by the simple thermal decomposition method.[19] The specific discharge capacity of V_2O_5 nanorods electrode is 270 mAh/g at a current density of 0.5 C, the cycle stability is good, and the cycle decay rate is only 0.32%. Even at a high current density of 4 C, the specific discharge capacity is 198 mAh/g. More oxalic acid was used to against aggregation and obtain more V_2O_5 nanoparticles. The shape of V_2O_5 nanoparticles shows a nanorod like structure with a width of 20–100 nm. This particle size is smaller than that of commercial. High porosity can improve specific capacity of LIB.

Hierarchical V_2O_5 nanobelts by chemical solid-state reaction, as shown in Fig. 2.[20] The structure can reduce the contact resistance between ions and materials, improve the volume change problem, and reduce the pressure of strong deformation during the charge/discharge process. It shows high specific capacity and excellent cycle stability. Specific capacity is 240 mAh/g at a current density of 1 C, and specific capacity is 174 mAh/g at a high current density of 8 C. In addition, after 100 cycles at a current density of 1 C, the capacity can maintain 91% of its initial capacity.

The 1D rod-shaped V_2O_5 was prepared with polyphenol grafted collagen fiber as a unique biological template.[21] This novel 1D rod-shaped structure has short the electron and ion transfer path. In addition, the oxygen vacancies are beneficial to the diffusion of lithium ions. Therefore, 1D rod like V_2O_5 has high specific capacity and excellent rate performance, with specific capacity of 255 mAh/g and 100 mAh/g at current densities of 0.1 C and 10 C.

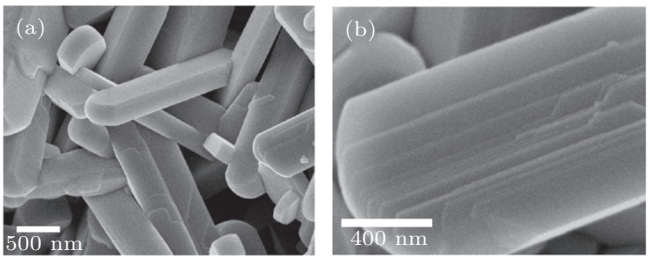


Fig. 2. SEM images of graded V_2O_5 nanobelts.[20]

The formation of V_2O_5 nanobelts may be related to the partial dissolution and recrystallization of V_2O_5 precursors.[22] Metastable VO_2(B) ultrathin nanobelts arrays were synthesized by template free hydrothermal method, and the porous V_2O_5 nanobelts arrays were obtained by sintering in air.[23] Porous nanobelts can provide high conductivity along the X–Y plane,[24] lithium ion diffusion and reduce electron transport distance. Electrolyte penetration and vol-

ume change is improve. When it is used as electrode material of LIB, it can provide 142 mAh/g initial specific capacity at 50 mA/g current density, and there is almost no capacity decay after 100 cycles. The ultra-thin porous structure of nanobelts determines its excellent electrochemical performance.

Hierarchical sisal like V_2O_5 microstructure[25] was synthesized by simple hydrothermal method using polyoxyethylene-20-hexadecyl ether as surface control agent. The microstructure is composed of primary 1D nanobelts with [001] oriented growth and oxygen vacancies. For V_2O_5, the surface energy of [001] surface is 0.22 J/m^2, which is the most stable surface of V_2O_5. The stable surface [001] can reduce reaction between electrode and electrolyte interface. 1D nanostructure can enhance the transport of electrons and ions.[26] In addition, the low valence vanadium can produce oxygen vacancies, which benefits the diffusion of lithium ions. The sisal like V_2O_5 microstructure provides high specific capacity of 297 mAh/g at 0.1 C current density.

In conclusion, the 1D V_2O_5 nanostructure is prepared by different methods. V_2O_5 nanorods (prepared by thermal decomposition method) exhibits the highest initial capacity, the porous nanobelts array have the highest capacity retention rate, and the hierarchical sisal like microstructure not only has high initial capacity, but also shows stable capacity retention.

2.2. The 2D nanostructure

The 2D leaf like V_2O_5 nanosheets were synthesized by a novel and green method, and the preparation process is shown in Fig. 3.[27] Its excellent high-speed performance comes from its unique structure, and mainly refers to the hierarchical porous structure and large specific surface area. It has good lithium storage performance in LIB, including high reversible capacity and high capacity retention. When the current density is 50 mA/g, 200 mA/g, 500 mA/g, 1000 mA/g and 2000 mA/g, the specific capacities are 303 mAh/g, 273 mAh/g, 251 mAh/g, 219 mAh/g and 160 mAh/g, respectively. Even at a very high current density of 5000 mA/g, it can still provide a specific capacity of 104 mAh/g. Due to the use of low-cost raw materials and simple experimental procedures, the method applies for industrial production.

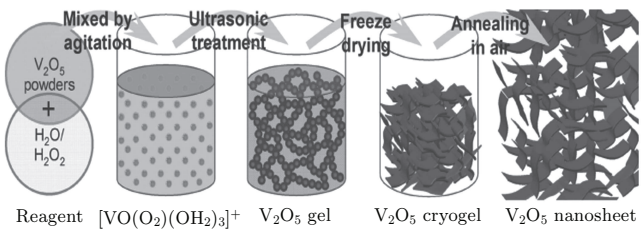


Fig. 3. Schematic diagram of the synthesis route of 2D leaf V_2O_5 nanoplates.[27]

The 2D V_2O_5 nanosheets with oxygen vacancies were prepared by hydrogenating V_2O_5 at relatively low temperature, which has good lithium storage performance.[28] Due to the large amount of oxygen vacancies, V_2O_5 nanosheets show high conductivity, fast lithium ion diffusion and high stability of lithium ion insertion/extraction structure, which gives it high capacity, rate capacity and cycle stability. The initial discharge specific capacity can reach 259 mAh/g when it is used as electrode material of LIB. When the current density increases from 0.1 A/g to 2 A/g, the initial discharge capacity decreases to 138 mAh/g at a current density of 2 A/g and the capacity retention rate is 55%. In addition, the V_2O_5 nanosheets have stable discharge capacity, and the discharge capacity attenuation of each cycle is less than 0.05%.

Multilayer V_2O_5 nanosheets with a thickness of 2.1–3.8 nm were prepared by directly stripping large V_2O_5 crystals in formamide solvent.[29] The ultra-thin thickness of V_2O_5 nanosheets provides a short diffusion path, and the unique nanostructure, which could improve the lithium ion and electron transfer rate, and receive high lithium insertion capacity and good cycle stability. The reversible specific capacity of the multilayer V_2O_5 nanosheets remains about 274 mAh/g after the 50th cycle at a current density of 0.2 C, which is equivalent to 93.8% of the initial capacity. Even at a current density of as high as 50 C, it still shows a specific capacity of 117 mAh/g after 200 cycles.

Xu Maowen *et al.* used a simple solvothermal method to synthesize V_2O_5 with a novel nested layered porous structure. The nested structure is about 1.5 μm in diameter, and consists of interconnected nanosheets with porous structures.[30] The electrode of V_2O_5 nanosheets shows excellent electrochemical performance. It can provide an initial discharge specific capacity of 330 mAh/g at a current density of 100 mA/g and maintains a stable discharge specific capacity of 240 mAh/g after 50 cycles. The excellent electrochemical performance is attributed to its layered porous structure, which can effectively buffer the local volume change and shorten the diffusion distance of lithium ions. Self-assembled V_2O_5 nanobelt films were prepared by Wang *et al.*[31] Nanobelt films of $V_2O_5{\cdot}xH_2O$ come from capsule self-assembly. When V_2O_5 nanobelt films were used as electrode materials for LIB, they showed excellent electrochemical performance and cycling stability.

In order to study the relationship between material size and capacity, the relationship of the specific capacity and nanomaterial sizes is showed in Fig. 4. It can be seen from Figs. 4(a) and 4(b) that the specific capacity increases quickly at first and then decreases with the increase of particle size, and the highest specific capacity appears at 90 nm of particle size. The relationship of particle size and capacity retention rate after 30 charge discharge cycles are given in Figs. 4(c) and 4(d). And the V_2O_5 nanobelts show low initial discharge capacity, they have a very high capacity retention rate and almost no capacity decay after 100 cycles. In addition, although the nano materials show high discharge capacity when the parti-

cle size is about 90 nm, the capacity retention rate is relatively low. Therefore, high capacity and capacity retention rate can be achieved by appropriate particle size of V_2O_5 nanomaterials.

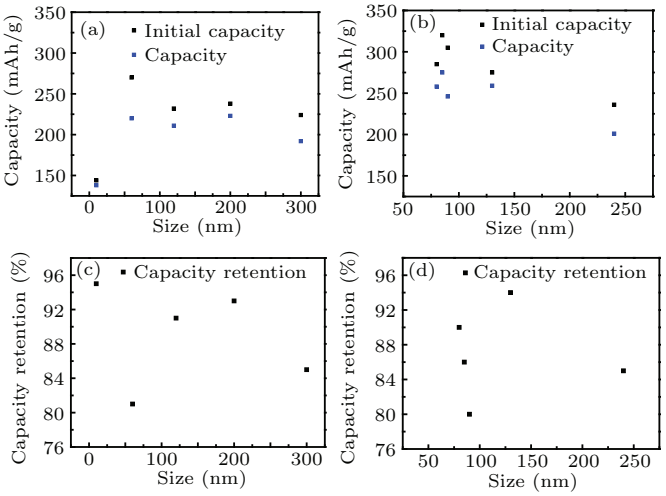


Fig. 4. (a) The relationship between the capacity and the size of 1D V_2O_5 nanomaterials. (b) The relationship between the capacity and the size of 2D V_2O_5 nanomaterials. (c) Relationship between capacity retention and nano size of 1D V_2O_5 nanomaterials after 30 cycles at 0.5 C current density. (d) Relationship between capacity retention and nano size of 2D V_2O_5 nanomaterials after 30 cycles at 0.5 C current density.

2.3. The 3D nanostructure

The 3D hollow porous quasi microspheres of V_2O_5 was successfully prepared by solvothermal method and annealing at 450 °C in air.[32] 3D nanostructures with internal vacancies can buffer volume expansion, reduce the stress and strain caused by insertion/extraction of lithium ions,[33,34] and provide shorter Li^+ diffusion distance. The quasi microspheres have good lithium storage performance, cycling performance, high specific capacity and good rate performance. The specific capacity of 173 mAh/g is obtained at a high current density of 2000 mA/g.

Hollow microspheres with multi shell/cavity of V_2O_5 were synthesized by catalytic burned process to remove carbon microsphere template.[35] Due to its unique structural characteristics, the thin three shell V_2O_5 hollow microspheres show extremely high specific capacity and excellent cycle stability at a current density of 1000 mA/g. The specific capacity the initial and after 100th cycle is 447.9 mAh/g and 402.4 mAh/g, respectively. Even when the current density is as high as 2000 mA/g, the specific capacity of 331.8 mAh/g can be obtained in Fig. 5.[35] The electrode composed of thin three shell V_2O_5 hollow microspheres has better electrochemical performance than other hollow structure or V_2O_5 nanoplates. The main reason is that three shell microspheres have a large specific surface area and pore volume, thus providing higher lithium storage location and increasing the channel of electrolyte penetration, which leads to a high specific capacity. In addition, the thin multi shell reduces the diffusion path, and thus shortens the diffusion time of lithium ion, as can be seen below:

$$t = L^2/D, \tag{1}$$

where t, L and D are diffusion time, diffusion length and diffusion constant, respectively.

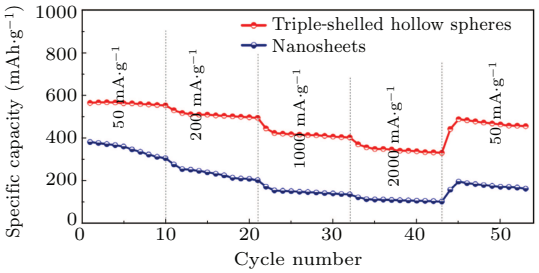


Fig. 5. Discharge curves of thin three shell V_2O_5 hollow microspheres and V_2O_5 nanosheets at different current densities.[35]

The 3D porous V_2O_5 hierarchical microspheres were synthesized by solvent heat method without additive and subsequent calcination.[36] The 3D porous V_2O_5 hierarchical microspheres are composed of porous nanofibers, which are aligned in a directional manner, thus forming a highly porous hierarchical structure. These V_2O_5 microspheres obtained an initial discharge specific capacity of 148 mAh/g at a current density of 0.5 C, and showed a stable capacity retention rate of 130 mAh/g in 100 cycles, and a capacity retention rate of 105 mAh/g even at a high current density of 30 C. The excellent electrochemical performance indicates that this unique V_2O_5 material is expected to be a cathode material for LIBs.

Porous V_2O_5 eggshell microspheres were prepared by the hydrothermal/solvothermal method.[37] Porous V_2O_5 eggshell microspheres help to provide high specific surface area and shorten the diffusion distance of lithium ions, thus speeding up the kinetic process of ion diffusion. The initial specific capacity of V_2O_5 eggshell microspheres is 287.2 mAh/g, and the specific capacity remains 225.7 mAh/g after 50 cycles at a current density of 50 mA/g. Even at the current density of 1000 mA/g, porous V_2O_5 eggshell microspheres can produce 117.5 mAh/g discharge capacity after 1000 cycles.

3D V_2O_5 hollow microspheres were synthesized by combining solvent heat treatment with subsequent annealing strategy.[38] Because the hollow structure can provide fast electrolyte transport and capacity adjustment, V_2O_5 microspheres electrode shows excellent rate performance and cycle stability. When it is used as electrode material of LIB, the initial discharge specific capacity of 273 mAh/g is achieved at current density of 0.2 C, and the specific capacity of 114 mAh/g is obtained even at a high current density of 8 C. The excellent lithium ion storage performance indicates that this unique V_2O_5 hollow material has a great prospect as an electrode for high-performance LIBs.

In order to obtain the relationship between the size and capacity of 3D materials, the relationship of the specific capacity and the capacity retention rate (after 30 charge discharge cycles) with the diameter of microspheres are shown in Fig. 6. From Fig. 6(a), we can see that the highest initial discharge capacity is achieved when the diameter of microspheres is about 1 μm. The capacity gradually decreases with the increasing of size. The capacity drops to 148 mAh/g when the diameter of the microspheres increases to about 12 μm. As shown in Figs. 6(a) and 6(b), the initial discharge capacity decreases with the increase of microsphere diameter, but the capacity retention rate decreases at first and then increases. Therefore, in the design of microsphere structure, it is also necessary to select the appropriate diameter of microsphere to make the electrochemical performance of nano materials better.

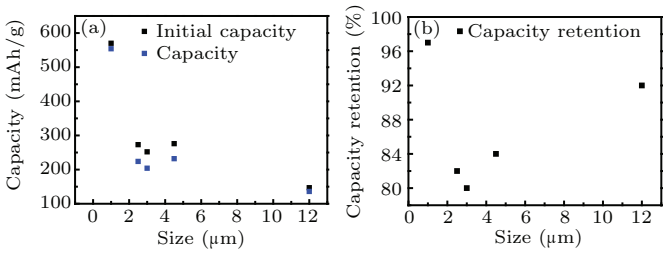


Fig. 6. Relationship of the capacity (a) and capacity retention (b) with the diameter of microspheres.

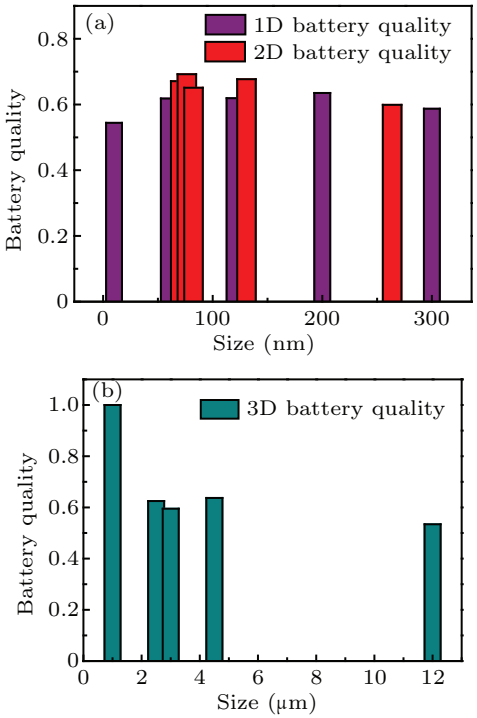


Fig. 7. Relationship between cell mass and nano size of 1D, 2D nano materials (a) and 3D nano materials (b).

In order to analyze the performance of various V_2O_5 nanomaterials as electrode materials for LIBs, we normalize the initial discharge capacity and capacity retention rate, as shown in Eq. (2). In 1D, 2D and 3D nanostructure materials, the highest initial discharge capacity and the highest capacity retention rate are taken as 1, and the remaining initial discharge capacity and capacity retention rate are divided by the highest initial discharge capacity and capacity retention rate, and then multiplied by 60% and 40% respectively and summed to get the index of battery quality, as shown in Fig. 7. Due to the large size of 3D nanomaterials, they are represented separately from 1D and 2D nanomaterials. The initial discharge capacity accounts for 60% of the battery mass, and the capacity retention rate accounts for 40% of the battery mass. The highest battery quality of 1D and 2D nanomaterial appears about 100 nm. The three-shell V_2O_5 hollow microspheres with a diameter of 1 μm show the highest battery quality in Fig. 7(b), and it has very high initial discharge capacity and excellent capacity retention rate. When the nano size is too large or too small, the battery quality is low

$$Q = \frac{C_1}{C_{1\max}} \times 0.6 + \frac{C_r}{C_{r\max}} \times 0.4. \tag{2}$$

3. Composite nanostructured of V_2O_5

This part mainly discusses the composite nanomaterials composed of V_2O_5 and different carbon carriers (such as graphene, carbon nanotubes and reticular porous carbon matrix), as shown in Table 3. Through different experimental strategies, the materials show different electrochemical properties.

3.1. V_2O_5/graphene composite material

Graphene nanobelts (GNRs) have been used as support materials for metal oxide composites in anode of LIBs.[39] A method of embedding nanocrystalline V_2O_5 in the 3D open framework of GNRs array to improve the conductivity of electrode is proposed, and V_2O_5/GNRs composites are obtained.[40] As a conductive network, the composites do not need any other carbon additives, and can be used as a platform to support V_2O_5 on its surface. By adjusting the mass ratio of GNRs to V_2O_5 nanoparticles, the high specific capacity is 278 mAh/g at 0.1 C current density, the capacity retention rate is more than 78% after 100 cycles, and specific capacity is 165 mAh/g at 2 C current density.

V_2O_5/GNS composites include ultra-long-ordered single-crystal V_2O_5 nanowires and large-scale continuous graphene nanosheets (GNS). The ultra-long V_2O_5 single-crystal nanowires are supported on transparent GNS substrate, and their SEM is shown in Fig. 8.[41] When the composites are used as electrode materials for LIBs, they exhibit high lithium ion storage performance, meanwhile high discharge capacity and stable rate performance are gained. At a low current density of 50 mA/g, V_2O_5/GNS composites can provide an initial discharge capacity of 412 mAh/g, even when the current density reaches 1600 mA/g, they can still achieve a specific capacity of 316 mAh/g.

Table 3. Electrochemical performance of carbonaceous materials used with V_2O_5 electrodes for LIB cathode materials.

Precursor material	Nanocomposites	Initial capacity (mAh/g)	Current density (mA/g)	Cycles (times)	Capacity (mAh/g)	References
VCl_4	Graphene	278	29.4	100	217	[40]
V_2O_5 powder	Graphene	277	294	50	179	[41]
–	Graphene	300	147	245	203	[42]
V_2O_5 powder	Graphene	225	2940	600	224	[43]
NH_4VO_3	Reduced graphene oxide	268	100	100	182	[44]
Ammonium metavanadate	MWCNT	265	29.4	100	187	[46]
V_2O_5 powder	CNT	240	1470	300	170.4	[47]
Vanadium oxytriisopropoxide	CNTs	158	5880	400	137	[48]
–	Networked porous carbon matrix	183	2940	5000	185	[49]
N, N-dimethylformamide	CNF	298	100	100	278	[50]
N, N-dimethylformamide	Carbon nanotubes	302	100	50	237	[51]
V_2O_5 powder	Mesoporous carbon	282	500	100	163	[52]

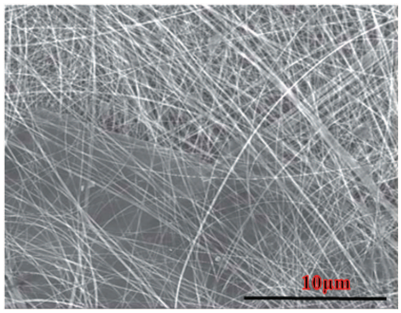


Fig. 8. SEM image of V_2O_5/GNS composites.[41]

Sandwich like ultra-thin V_2O_5@GNS are prepared by a simple method.[42] V_2O_5 nanosheets exhibit excellent high reversible capacity, cycle stability and high-rate performance as electrode materials for LIBs, which come from the rapid ion transport of ultra-thin V_2O_5 nanosheets and the excellent conductive platform of GNS. The initial reversible specific capacity of 300 mAh/g was achieved at a current density of 0.5 C. After 245 cycles, the specific capacity of 203 mAh/g was still maintained. Even at a high current density of 10 C, the specific capacity was 165 mAh/g.

Single-layer V_2O_5 nanobelts/graphene heterostructures were obtained by a simple and novel bottom-up method. The thickness of single-layer V_2O_5 nanobelts is 800 pm and the width is 80 nm, and they are connected with graphene as sandwich heterostructures by layer-by-layer assembly.[43] The V_2O_5 nanobelts/graphene heterostructures can significantly shorten the diffusion path of Li^+ and improve the conductivity of the electrode. When it is used as electrode materials for LIBs, it shows excellent reversible capacity and stable cycling performance, and has the rate characteristics similar to supercapacitor. At a current density of 10 C, the electrode has a high initial discharge specific capacity of 225 mAh/g and a capacity retention rate of 94.7% after 200 charge discharge cycles.

Surface modification was used to prepare $V_2O_5 \cdot nH_2O$ /reduced graphene oxide composites.[44] Due to the synergistic effect between 1D $V_2O_5 \cdot nH_2O$ nanoribbons and 2D rGO nanoplates, they provided short transport path and enhanced conductivity, and showed excellent electrochemical performance. When they are used as an electrode material, the reversible capacities of 268 mAh/g and 196 mAh/g are achieved at 100 mA/g and 1000 mA/g current density, respectively. And the capacity of 129 mAh/g is still maintained even at high current density of 2000 mA/g.

The relationship between capacity and capacity retention rate with nano size of V_2O_5/graphene composites are shown in Fig. 9. From Fig. 9(a), it can be seen that it has the highest initial discharge capacity and 91% capacity retention after cycling when the nano size of the composite is about 15 nm. With the increase of nano size to about 200 nm, the discharge capacity decreases to 225 mAh/g, and the capacity retention rate is 89%. By comparing Figs. 9(a) and 9(b), it can be found that when the initial capacity of the composite is high, its capacity retention rate is relatively low. Therefore, we should hardly study to improve the initial capacity and capacity retention rate.

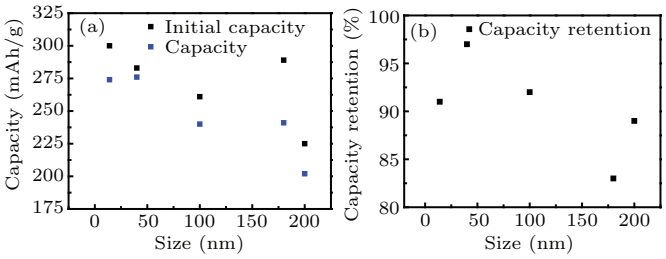


Fig. 9. (a) The relationship between the capacity and nano size of V_2O_5/graphene composites. (b) Relationship between capacity retention and nano size of V_2O_5/graphene composites after 30 cycles at 0.5 C current density.

3.2. V_2O_5/carbon nanotube composite

In order to further reduce the electron transport distance, V_2O_5 can be directly deposited on the surface of carbon nanotubes. Commercial carbon nanotubes (CNT) were coated with 4–5 nm V_2O_5 by solution hydrolysis method, creating an interpenetrating network of CNT and V_2O_5 nanowires.[45] However, the mass content of V_2O_5 achieved by this method

was limited, resulting in poor cycling performance of the materials.

Ethylene glycol was used as a green solvent to assemble V_2O_5 nanosheets onto multi walled carbon nanotubes (MWCNT) by one-step solvothermal method.[46] The *in-situ* formation of vanadium carbonate from ammonium metavanadate (NH_4VO_3) is an important step in the formation of V_2O_5/MWCNT composites, and then V_2O_5 and MWCNT self-assembly is driven by electrostatic interaction. 265 mAh/g high discharge capacity is achieved at 0.1 C current density. After 200 cycles, the discharge capacity is 133 mAh/g at 1 C current density, and the capacity retention rate is 78%, which shows long-term cycle stability and power capacity.

Ice template method was used to integrate banded V_2O_5 nanoparticles and CNT into 2D porous flake V_2O_5-CNT nanocomposites, and the SEM images are shown in Fig. 10.[47] The nanocomposites have unique structural characteristics, including 2D porous structure, large specific surface area and internal conductive network, and the excellent electrochemical performance in cycle stability and rate capacity is ensured when it is used. The discharge specific capacities of V_2O_5-CNT nanocomposites are 240 mAh/g, 180 mAh/g and 160 mAh/g at high current densities of 5 C, 10 C and 20 C, respectively. In addition, after 300 cycles at a high current density of 5 C, 71% of the initial discharge capacity is still retained and only 0.097% is lost per cycle.

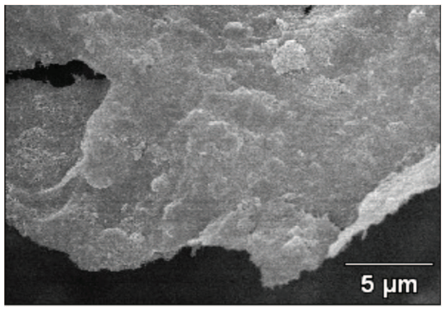


Fig. 10. SEM image of V_2O_5-CNT nanocomposites.[47]

Highly interconnected framework of V_2O_5 nanosheets and CNT were success- fully prepared by simple hydrothermal treatment and subsequent calcination process.[48] Sufficient space for the volume change during Li^+ insertion/extraction was provided by CNT and 2D V_2O_5 nanosheets, which can accelerate the kinetic process of ion diffusion, and gain high conductivity and structural stability. Due to the unique structural characteristic of CNT@V_2O_5, it shows excellent electrochemical properties. At a high current density of 20 C, it has a capacity of 137 mAh/g after 400 cycles. When the current density increases to 30 C, it still maintains a capacity of 116 mAh/g. The excellent electrochemical properties show that it has a broad prospect as a cathode material for LIBs.

3.3. V_2O_5/carbon matrix composite

A carbon fiber containing V_2O_5 nanoparticles encapsulated on a 3D mesh porous carbon matrix (V_2O_5/3DC-CFS) was reported by Zou *et al*.[49] In this design, the electrolyte is only in contact with the carbon skeleton, and can not contact with the internal V_2O_5 particles, which can reduce the formation of solid electrolyte interface (SEI) on the surface of V_2O_5 nanoparticles. In addition, 3D mesh porous carbon can effectively load V_2O_5 nanoparticles and provide a wide range of reaction sites. The special material composition and structure design make it in the voltage range of 4.0–2.0 V, and it still has a reversible specific capacity of about 183 mAh/g at a high current density of 10 C.

Core-shell structure composite of CNF-V_2O_5 was prepared by pulse electrodeposition from V_2O_5 sol solution and coating thin V_2O_5 layer on carbon nanofibers (CNF).[50] The uniform V_2O_5 shell with thickness of 30–50 nm formed a close interface with CNF core. The V_2O_5 shell in the composite has reversible $2Li^+/V_2O_5$ insertion/extraction, and the specific capacity of 291 mAh/g in the votage range of 4.0–2.0 V, which is close to its theoretical specific capacity. There is almost no capacity decay after 100 cycles, and it also has excellent stability at high rate. In addition, when the potential range is extended to 4.0–1.5 V, it corresponds to reversible $3Li^+/V_2O_5$ insertion/extraction, resulting in a high specific capacity of 429 mAh/g and a capacity retention rate of 70% after 100 cycles.

Carbon supported V_2O_5 hollow nanotube was prepared by solvothermal reaction and calcination using carbon fiber (CNF) as template.[51] By optimizing the reaction temperature, a clear nanotube morphology was synthesized. After annealing, both C and V^{4+} exist in the hollow nanotubes, which is beneficial to improve the conductivity. In addition, V_2O_5 nanotubes have high specific surface area, which is helpful to enlarge the contact area between electrolyte and electrode. When V_2O_5 nanotubes were used as cathode materials, the specific capacities of 237 mAh/g and 109.6 mAh/g were obtained at the current densities of 100 mA/g and 5000 mA/g in the voltage range of 2.0–4.0 V after 50 cycles, respectively.

Mohamed *et al.* prepared mesoporous carbon, and then prepared V_2O_5/mesoporous carbon composite by ultrasonic assisted sintering method.[52] The preparation method of mesoporous carbon is similar to that reported by Xue Jiafu *et al.*,[53] and ultrasonic treatment can effectively inhibit the aggregation of V_2O_5 particles. Because the mesoporous structure of V_2O_5/mesoporous carbon composite helps the electrolyte to diffuse into the main body of electrode materials, it can provide a fast channel for lithium ion transport, and the V_2O_5/mesoporous carbon composite has good electrochemical performance. At a current density of 500 mA/g, its capac-

ity is about 163 mAh/g after 100 cycles, and it has a higher charge discharge capacity than V_2O_5 nanoparticles.

After 30 cycles at a current density of 0.5 C, the relationship of the capacity and the relationship between the capacity retention rate with the nano size of V_2O_5/CNT and V_2O_5/carbon matrix composite are shown in Fig. 11. When the nano size of the composite is about 4 nm, it shows an initial discharge capacity of 275 mAh/g, but its capacity retention rate is relatively low. When the nano size increases to about 500 nm, it can be seen from Fig. 11(b) that the capacity retention rate decreases significantly. Therefore, when the nano size is about 80 nm, it shows high initial discharge capacity and excellent capacity retention.

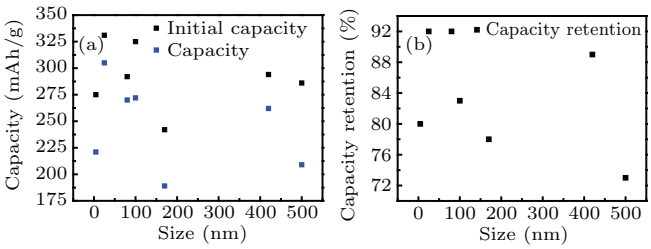


Fig. 11. (a) The relationship between the capacity and the nano size of V_2O_5/CNT and V_2O_5/carbon matrix composite. (b) The relationship between the capacity retention and the nano size of V_2O_5/CNTs and V_2O_5/carbon matrix composite.

The initial discharge capacity and capacity retention rate of V_2O_5/graphene, V_2O_5/carbon nanotube and V_2O_5/carbon matrix composite were normalized. The highest initial discharge capacity and capacity retention rate were 331 mAh/g and 98%, respectively, as shown in Fig. 12. The battery quality can be obtained by Eq. (2). When the nano size of the composite is less than 100 nm, the battery quality is high, especially the V_2O_5/3DC-CFS composite, which achieves a high discharge capacity of 331 mAh/g at a current density of 0.5 C. When the nano size is 100 nm, the battery quality of V_2O_5-CNT nanocomposites are better than that of $V_2O_5 \cdot nH_2O$ nanobelts/rGO composites. In addition, when the nano size is about 200 nm, the battery quality of the composite material decreases.

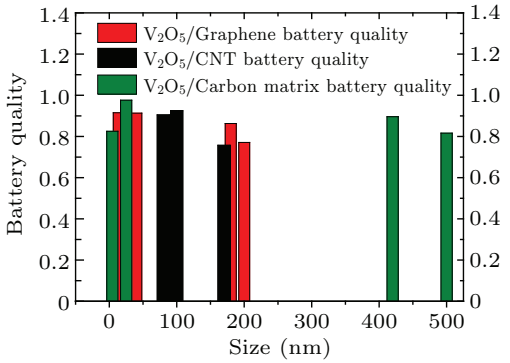


Fig. 12. Relationship between battery mass and nano size of three V_2O_5 Composites.

4. Cation doped V_2O_5

It is one of the common strategies to improve the electrochemical performance of V_2O_5 by doping. Table 4 summarizes the electrochemical properties of the cation doped V_2O_5 samples. Doping M element has the following different characteristics:[54] (1) Cation doping causes the formation of low valence V cations (V^{4+} and V^{3+}) to improve the electronic conductivity. (2) The addition of metal ions can form [MO_6] octahedral unit structure, which can stabilize the layered structure of V_2O_5 when Li^+ is insertion/extraction, and make it have better structural stability in the process of electrochemical cycling. (3) The local structural defects caused by external metal cations can be used as the nucleation center of the phase transition caused by the Li^+ insertion/extraction process, thus improving the electrochemical cycle stability of V_2O_5 electrode. In addition, these structural defects can provide more paths for the diffusion of Li^+. (4) The doping of cations reduces the charge transfer resistance and accelerates the kinetic process of Faraday reaction.

Table 4. The electrochemical properties of the cation doped V_2O_5 samples.

Precursor material	Doped metal	Initial capacity (mAh/g)	Current density (mA/g)	Cycles (times)	Capacity (mAh/g)	References
V_2O_5 powder	Ce	280.7	147	200	193.7	[57]
NH_4VO_3	Cu	289	294	50	254	[58]
NH_4VO_3	Co	281	500	100	264	[62]
V_2O_5 powder	Y	223	200	100	199	[67]
V_2O_5 powder	Ag	301	294	200	282	[68]
NH_4VO_3	Fe	257	58.8	50	188	[69]
V_2O_5 powder	Al	218	150	50	183	[70]

Cerium (Ce) is one of the most abundant rare earth elements, which has relatively large ionic radius and affinity for oxygen. It is usually selected as a structural stabilizer to improve the ionic conductivity.[55,56] Ce doped V_2O_5 microspheres were prepared by one-step solvothermal process and annealing. The results show that Ce doping can significantly improve the electrochemical performance of V_2O_5 microspheres.[57] $Ce_{0.1}V_2O_5$ microspheres have high initial reversible specific capacity of 280.7 mAh/g at 0.5 C and excellent specific capacity of 163.1 mAh/g at 10 C. The dis-

charge specific capacity of $Ce_{0.1}V_2O_5$ microspheres can be maintained as high as 193.7 mAh/g. Even after 200 cycles, the capacity retention rate is still about 88.93%, showing good cycle stability. The reason for the improvement of the electrochemical performance of Ce doped V_2O_5 microspheres is that the lattice expansion of Ce doped V_2O_5 microspheres can enhance the Li^+ diffusion coefficient of the electrode.

Rod like copper Cu doped V_2O_5 was synthesized by a simple solid-state chemical route.[58] The solid-state synthesis route has the characteristics of solvent-free and mild experimental conditions for the synthesis of inorganic nanomaterials.[59–61] Cu doping not only increases the cell volume, but also introduces a large number of oxygen vacancies in V_2O_5 lattice, which is conducive to the rapid migration of electrons and ions in the process of charging and discharging. In addition, it can inhibit the crystal growth, so that the length of Cu doped rod is reduced, which is beneficial to the full contact between electrode and electrolyte, and further improve the electrochemical performance. It shows a high discharge capacity of 293.1 mAh/g at 1 C, it is much higher than 235.5 mAh/g of undoped V_2O_5 and almost reaches the theoretical capacity of 294 mAh/g.

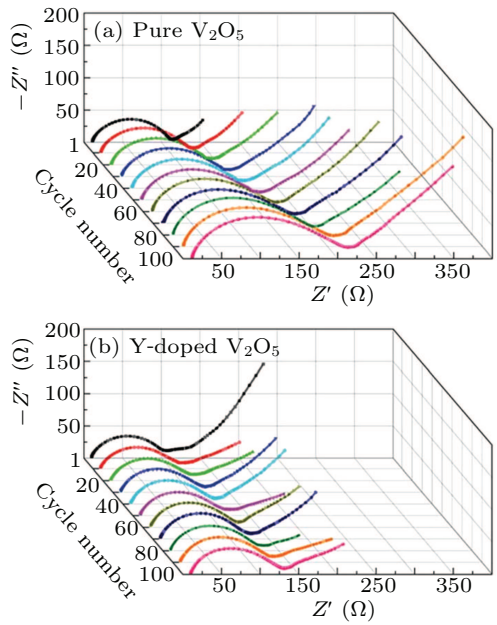


Fig. 13. Nyquist plots of the (a) pure V_2O_5 and (b) Y-doped V_2O_5 electrodes after various discharge/charge cycles.[67]

Cobalt Co doped V_2O_5 nanowire arrays were prepared by a simple hydrothermal method by controlling the appropriate molar ratio of cobalt acetate and ammonium vanadate.[62] When Co doped V_2O_5 nanowire arrays are used as electrode materials, they show high electrochemical lithium storage capacity. The initial discharge capacity of 624.64 mAh/g is obtained in the voltage range of 2–4 V at a current density of 30 mA/g. The good electrochemical performance can be attributed to the following factors: Co doped V_2O_5 nanowire arrays have higher electronic conductivity, which reduce the strain of Li^+ insertion/extraction and slow down the structural degradation.[63,64] Deep charging and discharging depth and dissolution of active substances in electrolyte are considered to be the main reasons for capacity degradation of vanadium oxide.[65]

The pure and Sn-doped V_2O_5 films were prepared by using the sol–gel method, followed by annealing at 450 °C for 2 h in air.[66] The Sn-doped V_2O_5 film electrode exhibits much enhanced electrochemical performances than the pure V_2O_5 counterpart. In particular, the Sn-doped V_2O_5 film shows much better cycle stability than the pure V_2O_5 film. Similarly, Y-doped V_2O_5 was prepared by the sol–gel method combined with the freeze drying technique followed by annealing in air.[67] Figure 14 gives the Nyquist plots of the pure V_2O_5 and Y-doped V_2O_5 electrodes after every ten discharge/charge cycles at the current density of 200 mA/g, respectively.[67] The R_{ct} of the pure V_2O_5 electrode increases rapidly with cycling, while that of the Y-doped electrode increases very slowly. The lower increase of impedance during cycling means smaller polarization and faster kinetics. When used as cathode material for LIBs, the Y-doped V_2O_5 exhibited much enhanced rate capability and cycling stability as compared to the pure V_2O_5 counterpart.

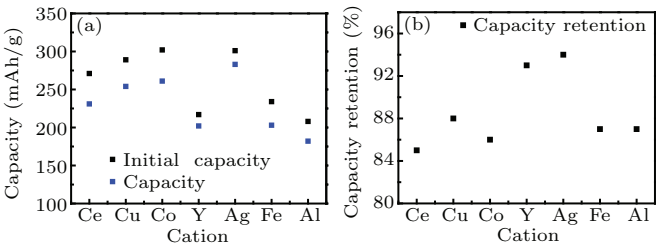


Fig. 14. (a) Capacity comparison of V_2O_5 nanomaterials doped with different cations. (b) Capacity retention of V_2O_5 nanomaterials doped with different cations after 50 cycles at 1 C current density.[57,58,62,67–70]

$Ag@V_2O_5$ nanosheet composites were prepared by a green liquid phase peeling (LPE) method.[68] The 2D ultrathin V_2O_5 nanosheets shorten the diffusion distance of Li^+ and realize face-to-face contact with the collector. The $Ag@V_2O_5$ nanosheets electrode exhibits high specific capacity of 301 mAh/g at a current density of 1 C. In addition, it also has excellent crystallinity and flexibility. When the $Ag@V_2O_5$ nanosheets electrode is bent at 180° for 100 times, and after the 200th cycle, its specific capacity can still be maintained at 233 mAh/g.

Carbon-free and binder-free porous V_2O_5 and $Fe_{0.1}V_2O_{5.15}$ thin films have been prepared by the electrostatic spray deposition technique.[69] The $Fe_{0.1}V_2O_{5.15}$ film shows much better capacity retention than the V_2O_5 film. The highly porous 3D structure can allow the electrolyte soaking well into the active material and facilitate the kinetics of Li^+ transport. After introducing Fe^{3+} into the V_2O_5 structure, the stability of the layered structure can be improved, leading to an improved cycling performance. After 48 cycles,

the $Fe_{0.1}V_2O_{5.15}$ electrode can still deliver a specific capacity of 195 mAh/g, which is 80% of the second-cycle discharge capacity.

V_2O_5 and $Al_{0.2}V_2O_5$ nanoparticles were prepared by an oxalic acid assisted soft-chemical method.[70] The cohesion between the V_2O_5 slabs was strengthened by Al^{3+} doping. This would be good for the electrochemical performance of the material from the structural point of view. The initial discharge capacity of the V_2O_5 nanoparticles was ~260 mAh/g. The material showed continuous capacity fading, which dropped below 140 mAh/g after 50 cycles. The $Al_{0.2}V_2O_5$ nanoparticles exhibited a smaller discharge capacity of ~220 mAh/g in the first cycle. The discharge capacity was 180 mAh/g after 50 cycles, which exhibited almost no capacity fading with respect to the third cycle.

The above cationic doped V_2O_5 nanomaterials are summarized as shown in Fig. 14. At a current density of 1 C, the prepared Ag@V_2O_5 nanosheet composites not only achieve the highest initial capacity, but also show an extremely high capacity retention rate after 50 cycles. In comparison, Y-doped V_2O_5 also have stable capacity retention, however the initial capacity is low. In the report of preparing Co doped V_2O_5 nanowire arrays, the highest current density is 500 mA/g when the electrochemical performance is tested. Therefore, it can be concluded that the composite electrode has no satisfactory electrochemical performance at high current density.

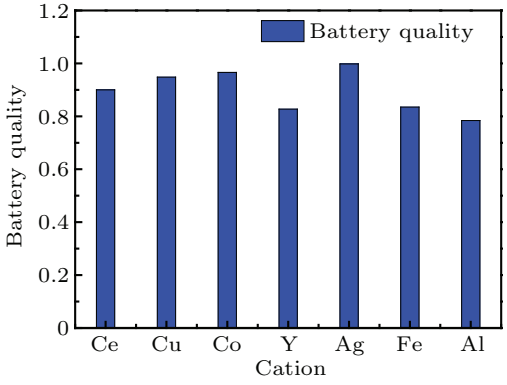


Fig. 15. Battery quality comparison of different cations doped V_2O_5 nanomaterials.

In order to study the performance of doped V_2O_5 nanomaterials for LIBs, the initial discharge capacity and capacity retention rate were also normalized by Eq. (2). Figure 15 shows the initial discharge capacity and capacity retention rate of cationic doped V_2O_5 nanomaterials. The highest initial discharge capacity and capacity retention rate are 302 mAh/g and 94%, respectively. Ag@V_2O_5 nanosheet composites exhibit the highest battery quality, the 2D ultra-thin V_2O_5nanosheets shorten the diffusion distance of Li^+ and realize face-to-face contact with the collector. Due to the additional Al^{3+} cations, which may occupy partial of the crystallographic sites that originally belong to Li^+, it makes $Al_{0.2}V_2O_5$ nanoparticles in low initial capacity and then causes it in low battery quality.

5. Conclusion

Among all the known electrode materials, V_2O_5 has the high reversible capacity, which is generally considered as a promising electrode material of LIB. Therefore, through the preparation and doping of V_2O_5 nanomaterials, the introduction of point defects in heterostructure crystal structure and the doping of cations, the electrochemical performance of V_2O_5 has been significantly improved in reversible capacity, high-rate capacity and long-term cycle stability, and the application prospect of V_2O_5 has become more extensive.

Nanostructures can greatly promote the electrochemical performance of V_2O_5 electrode materials. This paper mainly introduces the synthesis of V_2O_5 based nanomaterials with different structures and chemical compositions. Different structures include 1D, 2D and 3D nanostructures, while different chemical compositions include V_2O_5/graphene composite, V_2O_5/carbon nanotube composite and V_2O_5/carbon matrix composite. Among them, 1D nanostructures include nanorods and nanobelts, 2D nanostructures include leaf like nanosheets, multilayer V_2O_5 nanosheets and highly porous interconnection nanosheets, and 3D nanostructures include hollow structures, porous nanostructures, porous eggshell microsphere structures, etc. Finally, the V_2O_5 electrode materials doped with cations are discussed, including Ce, Cu, Co, Y, and other metal cations, which improve the performance of V_2O_5 electrode materials in different degrees. Through the observation and comparison of V_2O_5 based nanomaterials with different structures and chemical compositions, the appropriate nanostructures and optimized chemical compositions are obtained.

Acknowledgements

Project supported by the National Natural Science Foundation of China (Grant Nos. 51702097 and U1804125) and the Key Scientific and Technological Research Projects of Henan Province, China (Grant No. 202102210222).

References

[1] Li Z, Moreau L and Arking A 2010 *Bull Am. Meteorol Soc.* **78** 53
[2] Lin Y, Li Y and Zhan X 2012 *Chem. Soc. Rev.* **41** 4245
[3] Garg S, Jain A K, Yang S, *et al.* 2020 *Eur. Phys. J. Spec. Top.* **229** 2527
[4] Wu J, Tan Z, Wang K Liang Y and Zhou J H 2021 *Sustainability* **13** 3098
[5] Jung J, Jung S, Lee J, Lee M and Kim H S 2021 *Energies* **14** 3001
[6] Sutrisno D, Rahadiati A, Rudiastuti A W, Dewi R S and Munawaroh 2020 *ISPRS Int. J. Geo-Inf.* **9** 525
[7] Lund J W, Freestod D H and Boyd T L 2011 *Geothermics* **40** 159
[8] Mathew V, Kim S, Kang J, Gim J, Song J, Baboo J, Park W, Ahn D, Han J, Gu L, Wang Y, Hu Y, Sun Y and Kim J 2014 *NPG Asia Mater.* **6** 138
[9] Duffner F, Kronemeyer N, Tübke J, Leker J, Winter M and Schmuch R 2021 *Nat. Energy* **6** 123
[10] Goriparti S, Miele E, Angelis F D, Fabrizio E D, Zaccaria R P and Capiglia C 2014 *J. Power Sources* **257** 421

[11] Kalluri S, Yoon M, Jo M, Park S, Myeong S, Kim J, Dou S X, Guo Z and Cho J 2017 *Adv. Energy Mater.* **7** 1601507
[12] Ryu H H, Park G T, Yoon C S and Sun Y K 2019 *J. Mater. Chem. A* **7** 18580
[13] Lai F, Zhang X, Wang H, Hu S, Wu X, Wu Q, Huang Y, He Z and Li Q 2016 *ACS Appl. Mater.* **8** 21656
[14] Chen Y C, Xie K, Pan Y, Zheng C M and Wang H L 2011 *Chin. Phys. B* **20** 28201
[15] Tron A, Yong N J, Si H O, Park Y D and Mun J 2017 *ACS Appl. Mater.* **9** 12391
[16] Wu S L, Zhang W, Song X, Shukla A K, Liu G, Battaglia V and Srinivasan V 2012 *J. Electrochem. Soc.* **159** A438
[17] Vernardou D, Drosos C, Kafizas A, Pemble M E and Koudoumas E 2020 *Molecules* **25** 5558
[18] Yue Y and Liang H 2017 *Adv. Energy Mater.* **7** 1602545
[19] Pan A Q, Zhang J G, Nie Z, Cao G Z, Bruce W Arey, Li G S, Liang S Q and Liu J 2010 *J. Mater. Chem.* **20** 9193
[20] Rong Y L, Cao Y L, Guo N N, Li Y Z, Jia W and Jia D Z 2016 *Electrochim. Acta* **222** 1691
[21] Jiang H J Chen H, Wei Y H, Zeng J M, Liu H, Zhang Y and Hu H 2019 *J. Alloys Compd.* **787** 625
[22] Rui X, Tang Y, Malyi O I, Gusak A, Zhang Y, Niu Z, Tan H T, Persson C, Chen X, Chen Z and Yan Q 2016 *Nano Energy* **22** 583
[23] Qin M L, Liang Q, Pan A Q, Liang S Q, Zhang Q, Tang Y and Tan X P 2014 *J. Power Sources* **268** 700
[24] Wang S H, Yu T, Li Y Q, Fu H Y and Sun C L 2019 *Mater. Res. Bull.* **111** 284
[25] Wu N T, Du W Z, Liu G L, Zhou Z, Fu H R, Tang Q Q, Liu X M and He Y B 2017 *ACS Appl. Mater. Interfaces* **9** 43681
[26] Wei Q, Xiong F, Tan S, Huang L, Lan E H, Dunn B and Mai L 2017 *Adv. Mater.* **29** 1602300
[27] Li Y W, Yao J H, Evan U, Yang J W, Huang Y X, Zhang M and Cao G Z 2013 *Adv. Energy Mater.* **3** 1171
[28] Peng X, Zhang X M, Wang L, Hu L S, Cheng S H S, Huang C, Gao B, Ma F, Huo K F and Chu P K 2016 *Adv. Funct. Mater.* **26** 784
[29] Rui X H, Lu Z Y, Yu H, Yang D, Hng H H, Lim T M and Yan Q Y 2013 *Nanoscale* **5** 556
[30] Xie C Y, Cheng C J, Yang J G, Hou J K, Liu D Y, Liu S G, Han J, Zhang Y and Xu M W 2016 *Ceram. Int.* **42** 16956
[31] Wang Y, Zhang H J, Siah K W, Wong C C, Lin J Y and Borgna A 2011 *J. Mater. Chem.* **21** 10336
[32] Mai L Q, An Q Y, Wei Q L, Fei J Y, Zhang P F, Xu X, Zhao Y L, Yan M Y, Wen W and Xu L 2014 *Small* **10** 3032
[33] Vu A, Qian Y Q and Stein A 2012 *Adv. Energy Mater.* **2** 1056
[34] Wang Z Y, Zhou L and Lou X W 2012 *Adv. Mater.* **24** 1903
[35] Wang J Y, Tang H G, Zhang L J, Ren H, Yu R B, Jin Q, Qi j, Mao D, Yang M, Wang Y, Liu P R, Zhang Y, Wen Y R, Gu L, Ma G H, Su Z G, Tang Z Y, Zhao H J and Wang D 2016 *Nat. Energy* **1** 2251
[36] Zhang C F, Chen Z X, Guo Z P and Lou X W 2013 *Energy Environ. Sci.* **6** 974
[37] Dou Y F, Liang X, Gao G H and Wu G M 2018 *J. Alloys Compd.* **735** 109
[38] Zhang X Y, Wang J G, Liu H Y, Liu H Z and Wei B Q 2017 *Materials* **10** 77
[39] Lin J, Peng Z W, Xiang C S, Ruan G D, Yan Z, Natelson D and Tour J M 2013 *ACS Nano* **7** 6001
[40] Yang Y, Li L, Fei H L, Peng Z W, Ruan G D and Tour J M 2014 *ACS Appl. Mater. Interfaces* **6** 9590
[41] Liu H M and Yang W S 2011 *Energy Environ. Sci.* **4** 4000
[42] Wu L J, Zhang Y, Fan L S, Zhang Q, Wang P X, Tian D, Zhang N Q and Sun K N 2018 *Energy Technol.* **6** 551
[43] Zeng J, Huang J D, Liu J, Xie T, Peng C Q, Lu Y K, Lu P J, Zhang R Z and Min J 2019 *Carbon* **154** 24
[44] Zhang Y J, Yuan X Y, Lu T, Gong Z W, Pan L K and Guo S W 2021 *J. Colloid Interface Sci.* **585** 347
[45] Sathiya M, Prakash A S, Ramesha K, Tarascon J M and Shukla A K 2011 *J. Am. Chem. Soc.* **133** 16291
[46] Partheeban T, Kesavan T, Vivekanantha M and Sasidharan M 2019 *Appl. Surf. Sci.* **493** 1106
[47] Cheng J L, Gu G F, Guan Q, Razal J M, Wang Z Y, Li X L and Wang B 2016 *J. Mater. Chem. A* **4** 2729
[48] Yu R X, Zhang C F, Meng Q, Chen Z X, Liu H K and Guo Z P 2013 *ACS Appl. Mater. Interfaces* **5** 12394
[49] Zou R J, Liu Q, He G J, Yuen M F, Xu K B, Hu J Q, Parkin I P, Lee C S and Zhang W J 2017 *Adv. Energy Mater.* **7** 1601363
[50] Brown E, Park S H, Elangovan A, Yuan Y, Kim J, Sun X S, Zhang X M, Wang G and Li J 2018 *Electrochim. Acta* **269** 144
[51] Liang X, Gao G H, Feng S Z, Du Y C and Wu G M 2019 *J. Alloys Compd.* **772** 429
[52] Ihsan M, Meng Q, Li L, Li D, Wang H Q, Seng K H, Chen Z X, Kennedy S J, Guo Z P and Liu H K 2015 *Electrochim. Acta.* **173** 172
[53] Xue C F, Tu B and Zhao D Y 2008 *Adv. Funct. Mater.* **18** 3914
[54] Yao J H, Li Y W, Masse R C, Uchaker E and Cao G Z 2018 *Energy Stor. Mater.* **11** 205
[55] Zhai Y J, Xu L Q and Qian Y T 2016 *J. Power Sources* **327** 423
[56] Kou L Q, Chen F J, Tao F, Dong Y and Chen L 2015 *Electrochim. Acta* **173** 721
[57] Chen P Y, Zheng G T, Guo G Z, Wang Z C, Tang J, Li S, Wen Z S, Ji S J and Sun J C 2019 *J. Alloys Compd.* **784** 574
[58] Zhang H Y, Rong Y L, Jia W, Chai H and Cao Y L 2019 *J. Alloys Compd.* **802** 139
[59] Hu J D, Jia W, Xie J, Cao Y L, Zhang X H and Jia D Z 2018 *CrystEngComm* **20** 6156
[60] Xu H, Xie J, Jia W, Wu G M and Cao Y L 2018 *J. Colloid Interface Sci.* **516** 511
[61] Lu X Y, Jia W, Chai H, Hu J D, Wang S Q and Cao Y L 2019 *J. Colloid Interface Sci.* **534** 322
[62] Ji Y S, Fang D, Wang C, Zhou Z, Luo Z P, Huang J and Yi J H 2018 *J. Alloys Compd.* **742** 567
[63] Zhang X F, Wang K X, Wei X and Chen J S 2011 *Chem. Mater.* **23** 5290
[64] Li H Q, He P, Wang Y G, Hosono E J and Zhou H S 2011 *J. Mater. Chem.* **21** 10999
[65] Liu D, Liu Y, Garcia B B, Zhang Q, Pan A, Jeong Y H and Cao G 2009 *J. Mater. Chem.* **19** 8789
[66] Li Y W, Yao J H, Uchaker E, Zhang M, Tian J J, Liu X Y and Cao G Z 2013 *J. Phys. Chem. C* **117** 23507
[67] Yao J H, Yin Z L, Zou Z G and Li Y W 2017 *RSC Adv.* **7** 32327
[68] Qi Y Y, Qin K Y, Jian Z L, Yang X, Jin W, Tan Y X, Zou Y J and Chen W 2019 *J. Mater. Sci.* **54** 12713
[69] Li S R, Ge S Y, Qiao Y, Chen Y M, Feng X Y, Zhu J F and Chen C H 2012 *Electrochim. Acta* **64** 81
[70] Zhan S Y, Wei Y J, Bie X F, Wang C Z, Du F, Chen G and Hu F 2010 *J. Alloys Compd.* **502** 92